CHAPTER II

REVIEW OF LITERATURE

1. The *Pachastrissa nux* sponge

Sponges are the most primitive of the multicellular animals that their cells are not arranged to form permanent tissues or organs. Their body plans range from simple through to complex produced by varying degrees of infolding of the body wall and complexing of water canals throughout the sponge. They are sessile animals with radial or no symmetry. The sponge identifications are primarily based on the morphological characters, including shape, color, distribution of surface pores, ornamentation of the surface, texture, structure and composition of the organic skeleton and water canal system, and the structure, composition, size and geometry of the inorganic skeleton (Hooper, 2000).

Sponges are classified in the phylum Porifera, which is composed of four classes (one completely extinct), 5 subclasses, 28 orders, 232 families and 977 valid genera. (Hooper, 2000). The four classes are Archaeocyatha, Hexactinellida (glass sponges), Demospongiae, and Calcarea (calcareous sponges). The Demospongiae is the most diverse sponge group that contains about 95% of living species. The sponge *Pachastrissa nux* is one of species in this group and its taxa is given by Hooper as follows

Phylum Porifera

Subphylum Cellularia

Class Demospongiae

Order Astrophorida

Family Calthropellidae Lenderfeld, 1906

Genus *Pachastrissa* Lenderfeld, 1903

Species *nux* (de Laubenfels, 1954)

The grayish black sponge collected from Sichang Island, Chonburi Province, Thailand, in February 2003 was identified as *Pachastrissa nux* by Dr. John N. A. Hooper. The voucher specimens have been deposited at the Queensland Museum, South Brisbane, Australia (QM G320226) and at the Department of Pharmacognosy, Faculty of Pharmaceutical Sciences, Chulalongkorn University, Bangkok, Thailand (SC 602-03). This sponge is encrusting and spreading over substratum with small blackish fistules growing from a massive partially burrowing base. The live sponge has greenish gray exterior color and whitish brown with black margin interior color. In ethanol, the color of this sponge is gray. Its texture is firm, brittle and harsh. The surface is membranous, opaque, slightly rough and corrugated. Ectosomal skeleton has dense layer of oxeas as upright brushes or paratangential to the surface. There is dense collagen and gramular in mesohyl. Choanosomal consist of oxeas of two size classes (1500-1700×25×40 μM and 230-740×12-19 μM) and small calthrops with longer single axial ray (50-100 μM) that all rays are equidistant.

2. Chemical constituents of the genus *Pachastrissa*

A small number of compounds have been isolated from the sponge in the genus *Pachastrisa*. These compounds were bengazole, bengamide, lactone, and sphingosine derivatives.

Bengazoles 1-11 **[1-11]** were isolated from a sponge *Pachastrissa* sp. from Musha Archipelago, Republic of Djibouti. Only bengazoles 1-10 were found to be very active against *Candida albicans*, with MIC values from 0.8 to 1.5 μg/mL (Fernández et al., 1999).

Bengamides A, B, E, F, and L **[12-16]** were also isolated from the sponge *Pachastrissa* sp. along with bengazoles (Fernández et al., 1999). Bengamides A and B showed cytotoxicity against some cell lines in the 60 cell lines screening assay by the National Cancer Institute-Development Therapeutics Program (NCI-DTP). The data are reported in Table 1 and the average IC_{50} values were 46 nM for bengamide A and 11 nM

for bengamide B. The cytotoxicity against MDA-MB-435 human mammary carcinoma was also determined for bengamides A, B, E, and F (Table 2) (Thale et al., 2001).

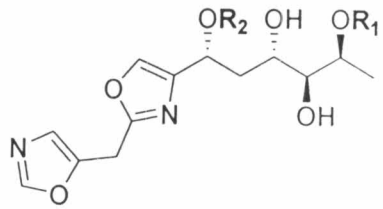

	R_1	R_2
[1]	$CO(CH_2)_{14}CH_3$	H
[2]	H	$CO(CH_2)_{14}CH_3$
[3]	$CO(CH_2)_{12}CH(CH_3)_2$	H
[4]	H	$CO(CH_2)_{12}CH(CH_3)_2$
[5]	$CO(CH_2)_{13}CH_3$	H
[6]	H	$CO(CH_2)_{13}CH_3$
[7]	$CO(CH_2)_{11}CH(CH_3)_2$	H
[8]	H	$CO(CH_2)_{11}CH(CH_3)_2$
[9]	$CO(CH_2)_{12}CH_3$	H
[10]	H	$CO(CH_2)_{12}CH_3$
[11]	H	H

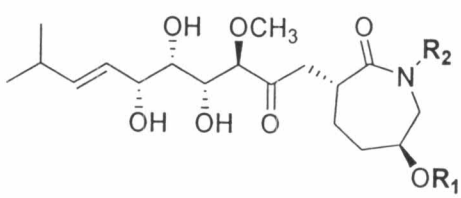

	R_1	R_2
[12]	$CO(CH_2)_{12}CH_3$	H
[13]	$CO(CH_2)_{12}CH_3$	CH_3
[14]	H	H
[15]	H	CH_3
[16]	$CO(CH_2)_{11}CH(CH_3)_2$	H

Table 1 The cytotoxicity of bengamides A and B.

Tumor type	IC_{50} (nM)	
	bengamide A [12]	bengamide B [13]
NSCL		
A549	19	1.9
HOP92	200	6.8
NCI-H522	60	6.3
Colon		
HCT116	18	2.4
HCT15	260	130
COLO205	18	25
CNS		
SNB75	190	63
SNB19	24	8.6
Melanoma		
UACC62	15	5.2
LOX IMVI	23	2.3
MALME-3M	180	22
Ovarian		
OVCAR3	10	10
OVCAR8	7	5.1
Renal		
UO31	370	25
786-0	24	3.5
Leukemia		
CCRF-CEM	27	7.3
Average IC_{50}	46 ± 5	11 ± 1

Table 2 The cytotoxicity against MDA-MB-435 human mammary carcinoma of bengamides A, B, E, and F

Compounds	IC_{50} (nM)
Bengamide A [12]	1 ± 0.6
Bengamide B [13]	12 ± 3
Bengamide E [14]	3300 ± 1200
Bengamide F [15]	2900 ± 2900

Together with bengamides and bengazoles, a lactone **[17]** was also isolated from the same *Pachastrissa* sp. sponge. (Fernandez et al., 1999)

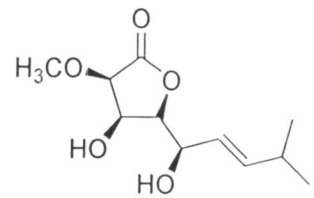

[17]

Pachastrissamine **[18]** was isolated from a sponge *Pachastrissa* sp. from Funauki Bay, Iriomote Island. This compound presented cytotoxicity against P388, A549, HT29 and MEL28 cell lines at a level of IC_{50} 0.01 µg/mL (Kuroda et al., 2002).

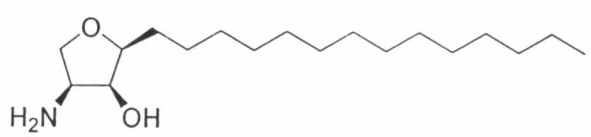

[18]

3. Trisoxazole macrolide compounds

The trisoxazole macrolides are a family of compounds that have related structures containing three contiguous oxazole containing macrolide ring and the extended terminal *N*-methyl formamide aliphatic tail. The compounds in this group are different mainly in various substitutions along the backbone. Trisoxazole macrolides have been isolated from nudibranch, nudibranch egg masses, sponges and stony coral and are widely recognized to have potent and diverse biological activities such as antifungal activity, cytotoxicity, icthyotoxicity and inhibition of cell division in the fertilized sea urchin eggs. Recently, a number of studies have reported that these trisoxazole macrolides bound tightly to G-actin with a stoichiometry of 1:1 (Saito et al., 1994; Wada

et al., 1998; Tanaka et al., 2003). The absolute stereochemistry of these large macrolides was determined using a combination of chemical degradation, extensive ^{1}H and ^{13}C NMR analysis, and X-ray crystallography (Matsunaga et al., 1999; Chattopadhyay and Pattenden, 2000; Klenchin et al., 2003; Allingham et al., 2004).

Ulapualides A and B **[19-20]**, isolated from the nudibranch *Hexabranchus sanguineus* eggmasses, inhibited L1210 leukemia cell proliferation at IC_{50} 0.01-0.03 µg/mL. Ulapualide A also showed antifungal activity against *Candida albicans* with a 17-mm zone of inhibition at the concentration of 0.4 µmol/disc (Roesener and Scheuer, 1986).

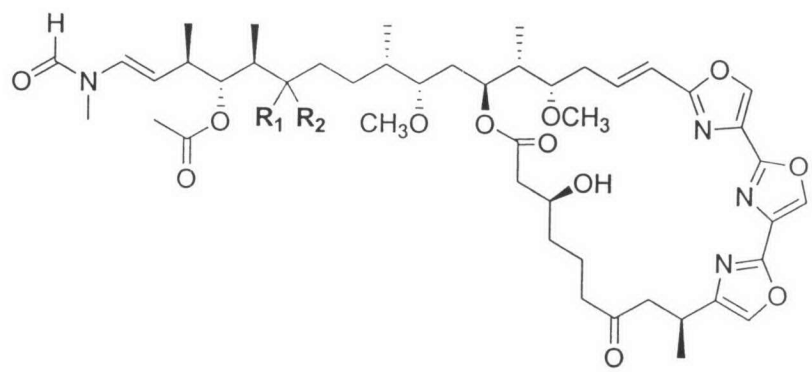

	R_1	R_2
[19]		=O
[20]	H	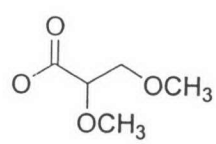

Kabiramides A-E **[21-25]** were obtained from the nudibranch *Hexabranchus* eggmasses (Matsunaga et al., 1986; 1989). Kabiramides B and C were also isolated from the sponge *Halichondria* sp. by Kernan and Faulkner (1987). Kabiramide C showed antifungal activity against *Candida albicans* ATCC 10234, *Aspergillus niger* ATCC 9642, *Penicillium citrium* ATCC 9849, and *Trichophyton interdigitae* with inhibition zones of 7.7, 30.7, 20.0, and 21.1 mm, respectively, using filter paper disc saturated with a 250 µg/mL solution of the compound (Matsunaga et al.,

1986). Kabiramides were strongly active in the sea urchin egg assay and also cytotoxic against L1210 cells (Table 3) (Matsunaga et al., 1989).

Table 3 The bioactivities of kabiramide compounds.

Compound	Sea urchin egg assay IC_{99} (μg/mL)	Cytotoxicity against L1210 cells IC_{50} (μg/mL)
Kabiramide A [21]	1.0	0.03
Kabiramide B [22]	0.2	0.03
Kabiramide C [23]	0.2	0.01
Kabiramide D [24]	0.2	0.02
Kabiramide E [25]	0.2	0.02

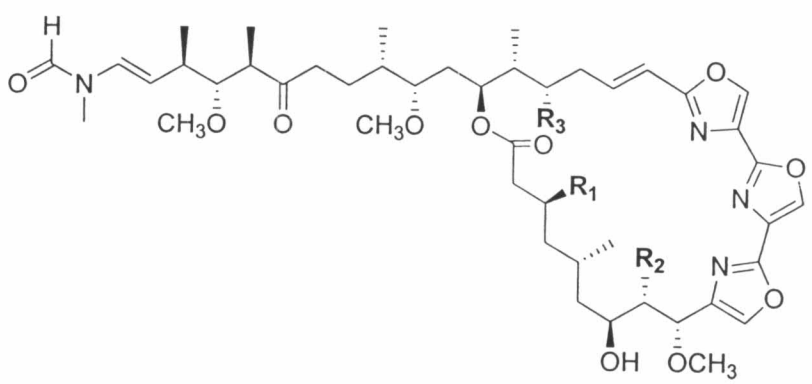

	R_1	R_2	R_3
[21]	$OCONH_2$	CH_2OH	OCH_3
[22]	$OCONH_2$	CH_3	OH
[23]	$OCONH_2$	CH_3	OCH_3
[24]	OH	CH_3	OCH_3
[25]	$OCOCH_3$	CH_3	OCH_3

Halichondramide [26], isohalichondramide [27], dihydrohalichondramide [28], halichondramide acid [29], halichondramide imide [30], and halichondramide ester [31] were isolated from the sponge *Halichondria* sp. and tetrahydrohalichondramide [32] was isolated from the nudibranch *Hexabranchus sanguineus*. The antifungal activity

and the inhibition of cell division in fertilized sea urchin egg are shown in Table 4. Furthermore, halichondramide caused mortality of mice via subcutaneous injection at the dose of 1.4 mg/kg (Kernan and Faulker, 1987; Kernan et al., 1988). The 33-methyldihydrohalichondramide [33] was obtained from the nudibranch *Hexabranchus* eggmasses by Matsunaga et al. (1989) and exhibited cytotoxicity against L1210 leukemia cells at IC_{50} 0.05 µg/mL. This compound was also strongly active in sea urchin egg assay at IC_{99} 0.5 µg/mL.

Table 4 The bioactivities of the halichondramides from the sponge *Halichondria* sp. and the nudibranch *Hexabranchus sanguineus*.

Compound	Sea urchin egg assay IC_{99} (µg/mL)	Antifungal against *Candida albicans*[a]
Halichondramide [26]	4	active
Isohalichondramide [27]	4	active
Dihydrohalichondramide [28]	1	active
Halichondramide acid [29]	less active	active
Halichondramide imide [30]	less active	less active
Halichondramide ester [31]	N/D[b]	less active
Tetrahydrohalichondramide [32]	1	active

[a]Disc diffusion method at concentration of 0.5 µg/disc

[b]No data

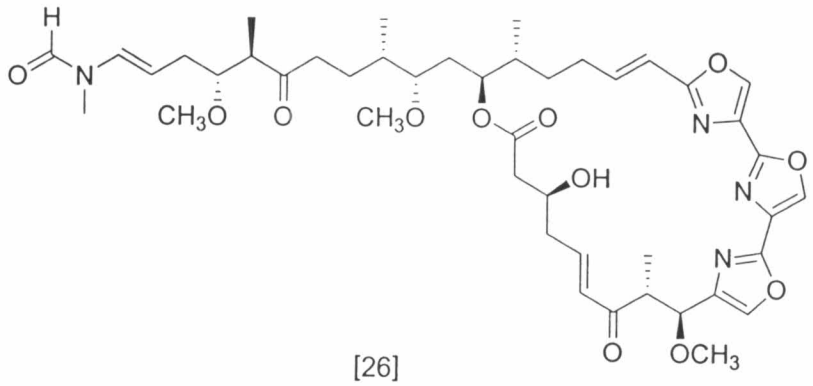

[26]

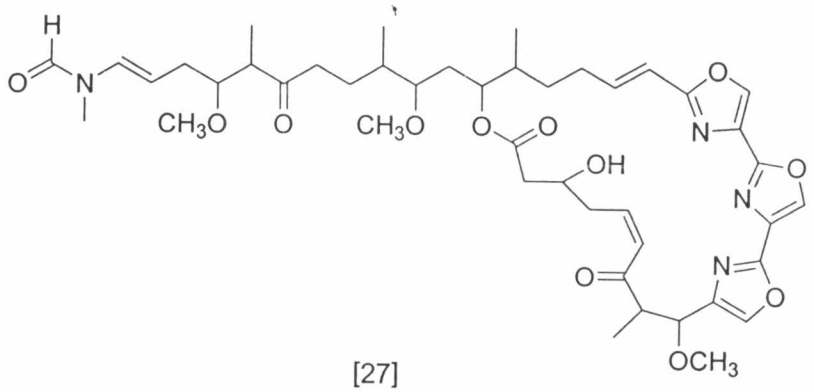

[27]

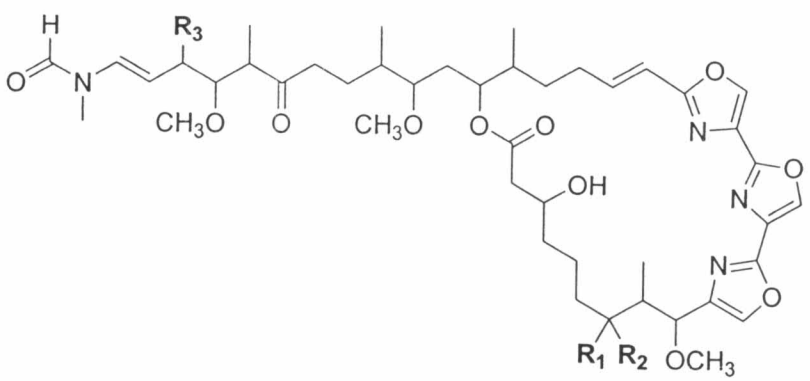

	R_1	R_2	R_3
[28]		=O	H
[32]	H	OH	H
[33]		=O	CH_3

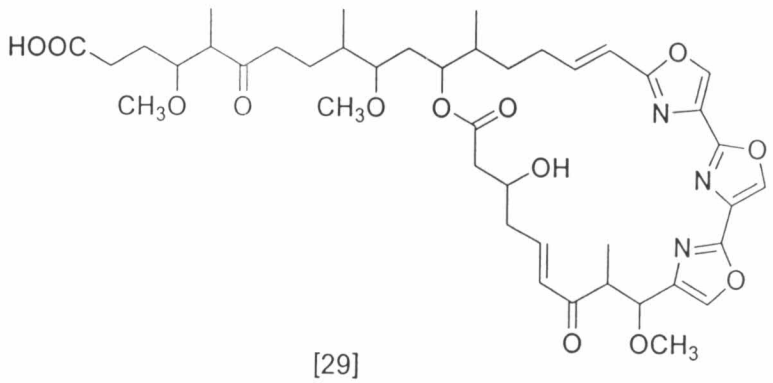

[29]

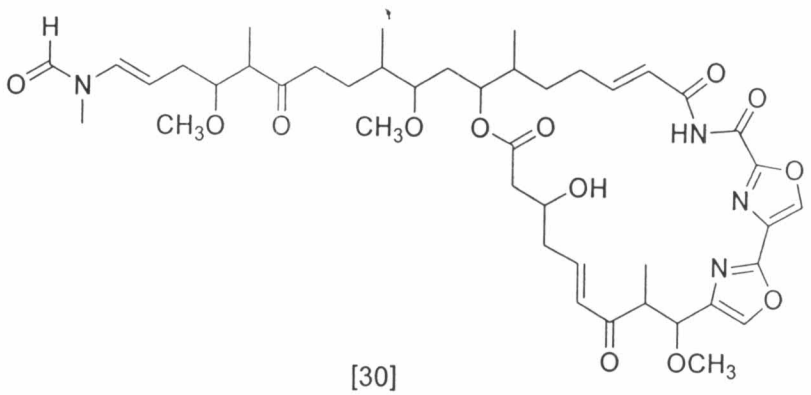

[30]

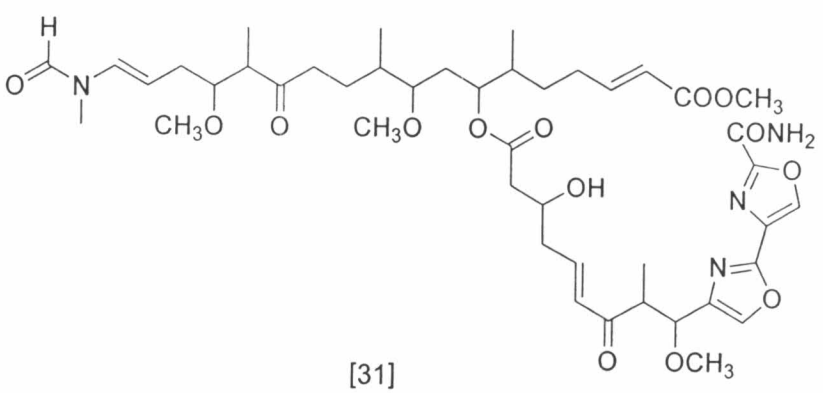

[31]

In 2004, Shin et al. reported the isolation of neohalichondramide **[34]**, (19*Z*)-halichondramide **[35]**, and secohalichondramide **[36]** from the sponge *Chondrosia corticata*. All compounds exhibited cytotoxicity toward the human leukemia cells K562 and antifungal activity against *Candida albicans* and *Aspergillus niger* (Table 5).

Table 5 The bioactivities of halichondramides from the sponge *Chondrosia corticata*.

Compound	Cytotoxicity against K562 cell line IC_{50} (μg/mL)	Antifungal activity[a]	
		Candida albicans (mm)	*Aspergillus niger* (mm)
Neohalichondramide **[34]**	0.38	20	15
19Z-Halichondramide **[35]**	0.90	10	10
Secohalichondramide **[36]**	>500	15	-

[a]The diameter of clear zone at the concentration of 2 μg/disc

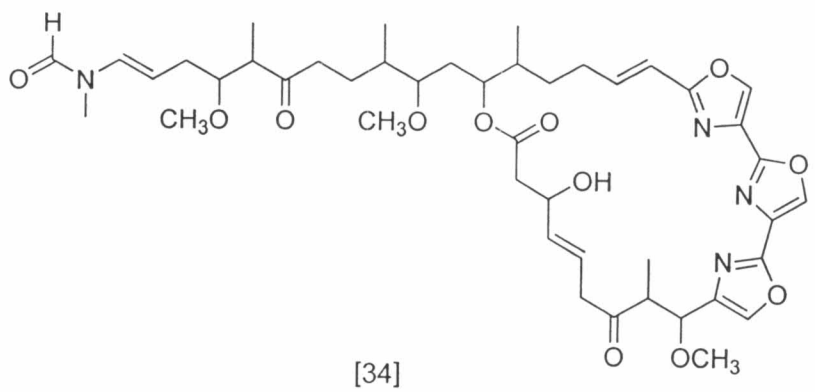

[34]

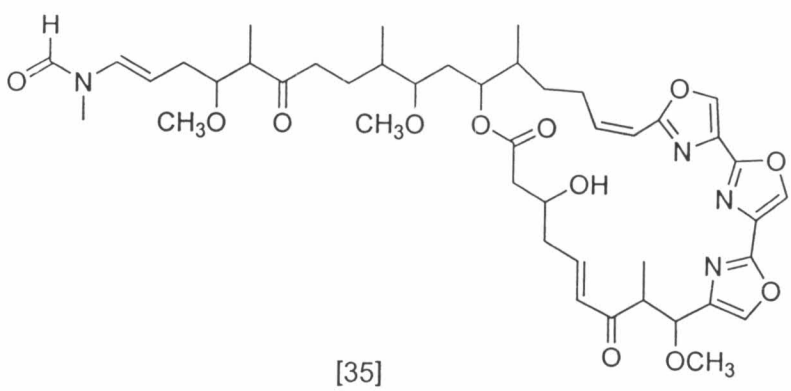

[35]

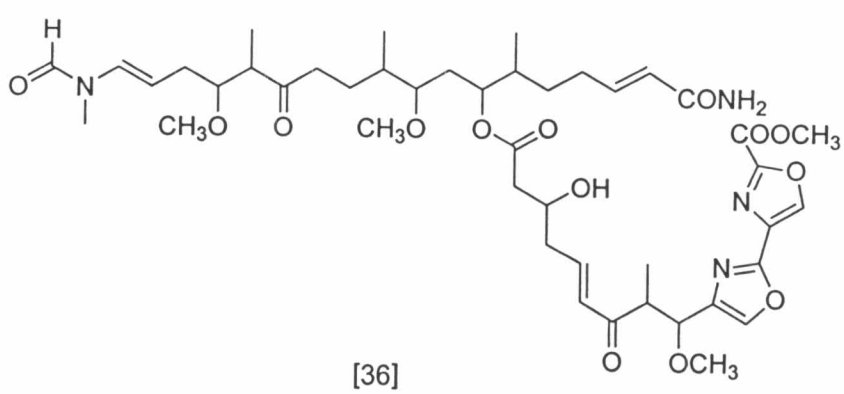

[36]

Mycalolides A-C [37-39], and thiomycalolides A and B [40-41] were isolated from the sponge *Mycale* sp. Mycalolides A-C showed antifungal activity against many fungi and cytotoxicity against B-16 melanoma cells with IC_{50} values of 0.5-1.0 ng/mL (Fusetani et al., 1989). Thiomycalolides A and B exhibited cytotoxic activity against P388 marine leukemia cells with IC_{50} of 18 ng/mL each (Matsunaga et al., 1998a). Matsunaga et al. (1998b) also reported the isolation of 30-hydroxymycalolide A [42], 32-hydroxymycalolide A [43], and 38-hydroxymycalolide B [44] from the sponge *Mycale magellanica*, which presented cytotoxic activity against L1210 leukemia cells with IC_{50} values of 19, 13, and 15 ng/mL, respectively. In 2002, 30,32-dihydroxymycalolide A [45] was obtained from the sponge *Mycale izuensis* and showed cytotoxic activity against HeLa cells with IC_{50} 2.6 ng/mL (Phuwapraisirisan et al., 2002). Mycalolides D and E [46-47] were found in the stony coral *Turbastrea faulkneri*, along with mycalolide C. Mycalolide D showed moderate cytotoxicity with average IC_{50} value of 0.6 μM in the NCI's 60 human tumor cell lines screening panel (Rashid et al., 1995).

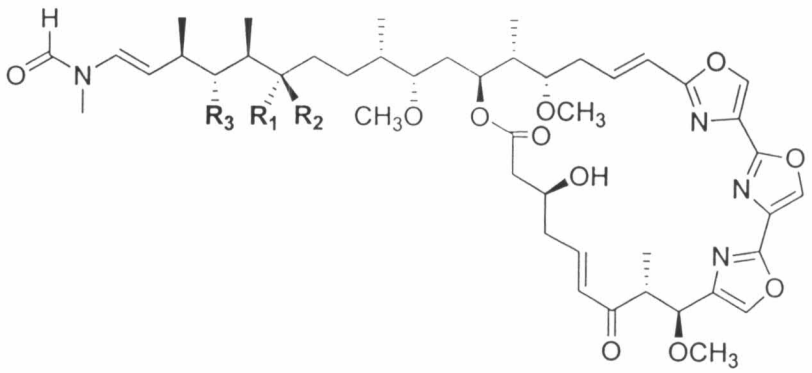

	R_1	R_2	R_3
[37]		=O	$OCOCH_3$
[38]	H	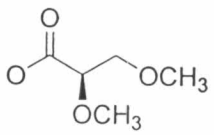	$OCOCH_3$
[39]	H	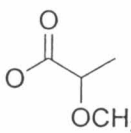	$OCOCH_3$
[42]	H	OH	$OCOCH_3$
[43]		=O	OH
[44]	H	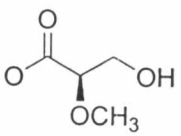	$OCOCH_3$
[45]	H	OH	OH

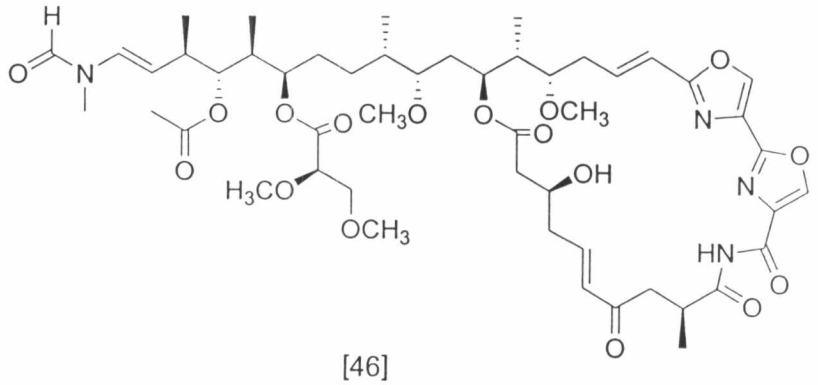

[46]

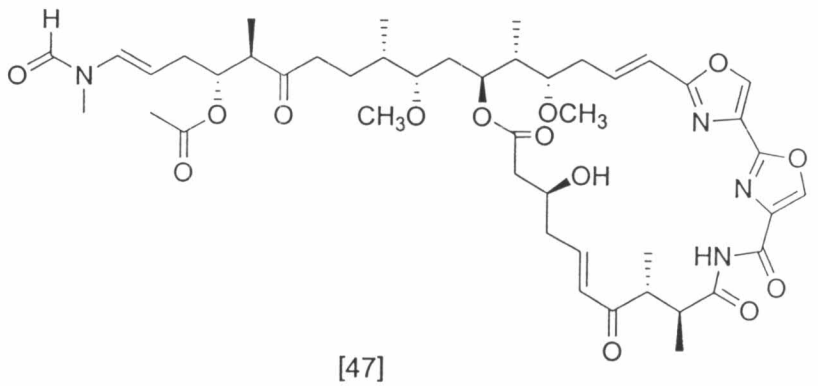

[47]

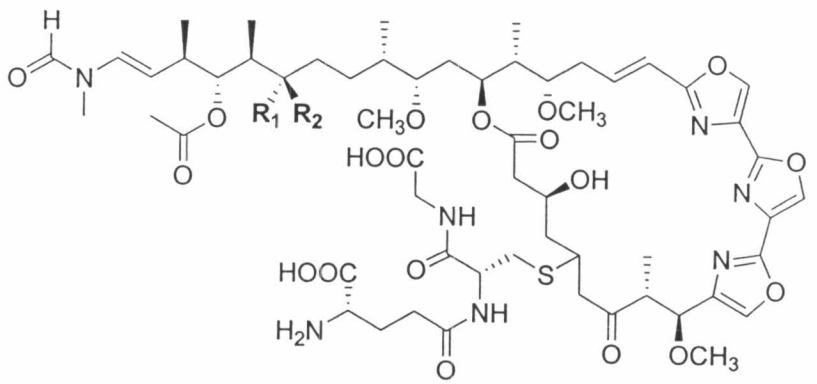

	R_1	R_2
[40]		=O
[41]	H	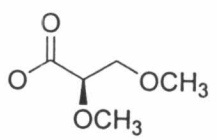

Jaspisamides A-C [48-50] were isolated from the sponge *Jaspis* sp., which exhibited cytotoxicity against L1210 murine leukemia cells and KB human epidermoid carcinoma cells as shown in Table 6 (Kobayashi et al., 1993).

Table 6 The bioactivities of the jaspisamides.

Compound	Cytotoxicity	
	L1210 cells (ng/mL)	KB cells (ng/mL)
Jaspisamide A [48]	<1	15
Jaspisamide B [49]	<1	6
Jaspisamide C [50]	<1	13

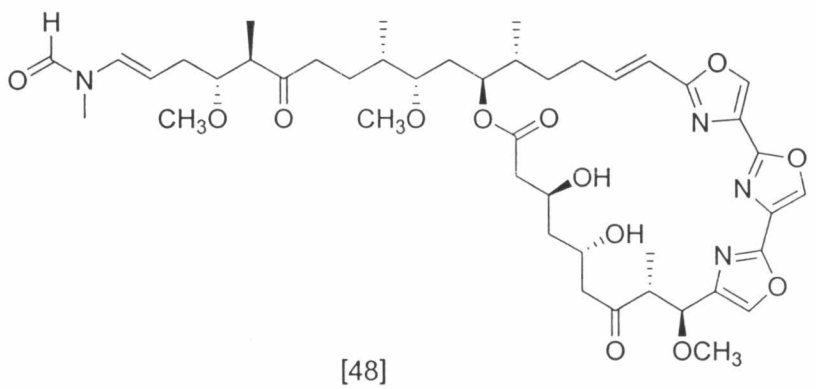

[48]

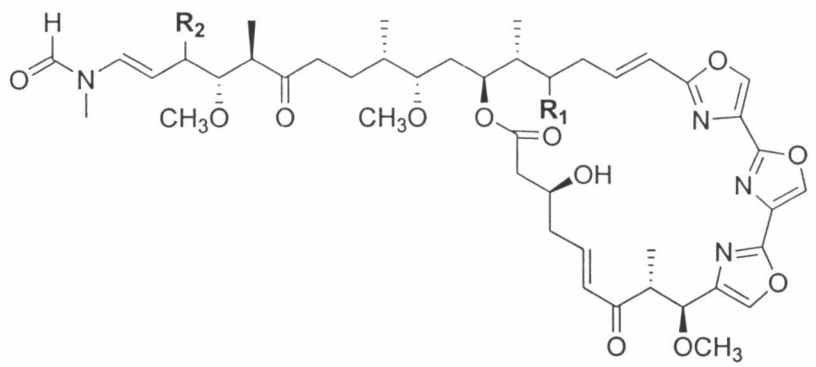

	R_1	R_2
[49]	OH	H
[50]	H	CH_3

Halishigamides A-D **[51-54]** were found in the sponge *Halichondria* sp. Halishigamide A exhibited potent cytotoxic activity against murine lymphoma L1210 and human epidermoid carcinoma KB cells, and antifungal activity against *Trichophyton mentagrophytes*. In contrast, halishigamides B-D had weak cytotoxicity against L1210 and KB cells, and modest antifungal activity against *T. mentagrophytes* (Table 7) (Kobayashi et al., 1997)

Table 7 The bioactivities of the halishigamides.

Compound	Cytotoxicity		Antifungal activity against *T. mentagrophytes* (MIC, μg/mL)
	L1210 cells IC_{50} (μg/mL)	KB cells IC_{50} (μg/mL)	
Halishigamide A **[51]**	0.0036	0.012	0.1
Halishigamide B **[52]**	4.4	7.5	25
Halishigamide C **[53]**	5.2	6.5	25
Halishigamide D **[54]**	1.1	1.8	6.5

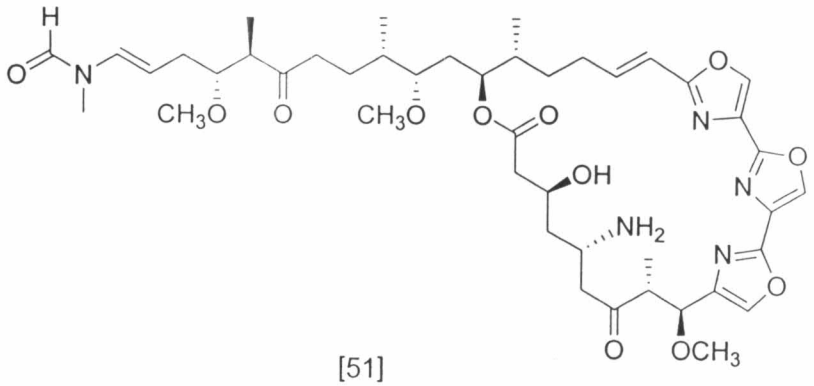

[51]

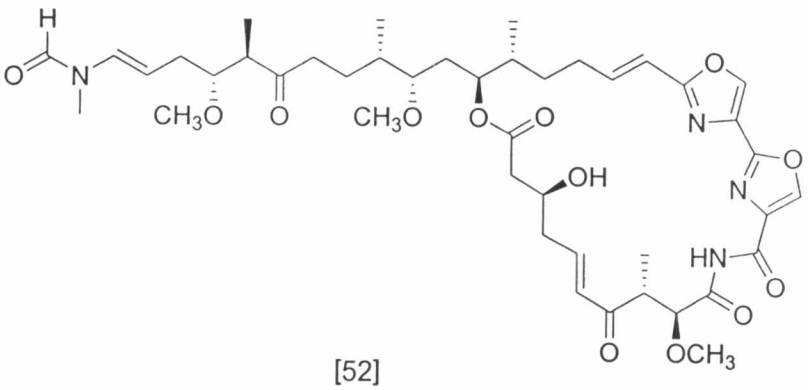

[52]

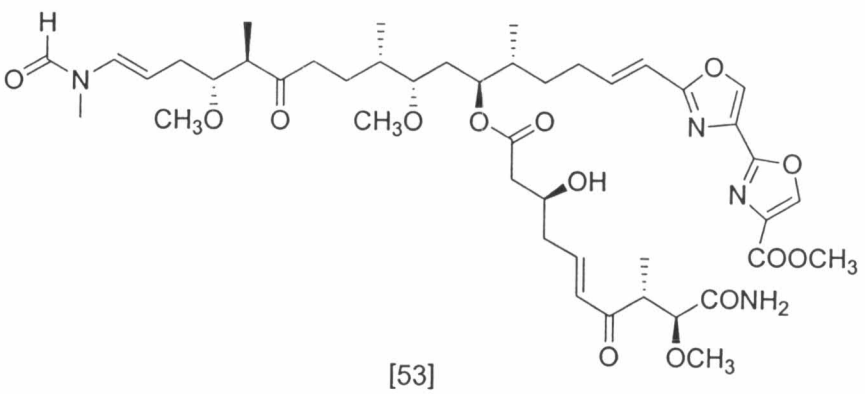

[53]

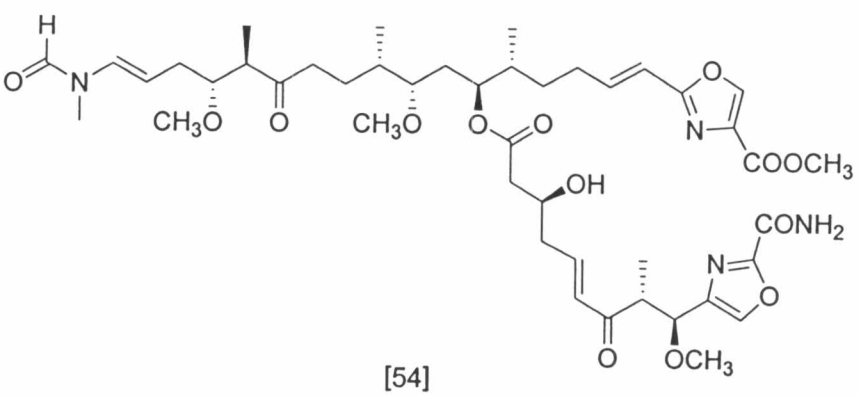

[54]

4. Actin cytoskeleton

Actin, a 42 kD protein, is one of the most abundant protein found in eukaryotic cells and highly conserved between species. It exists as a globular monomer (G-actin) or as a filament (F-actin). The monomeric actin, a slow ATPase, is composed of a 375 amino acid polypeptide chain and interacts with one molecule of ATP or ADP. A hypothetical vertical line divides the actin molecule into two domains: large and small. Both domains consist of two subdomains: the small domain is composed of subdomains 1 and 2, and the large domain of subdomains 3 and 4 (Figure 1) (Holmes et al., 1990; Otterbein et al., 2001).

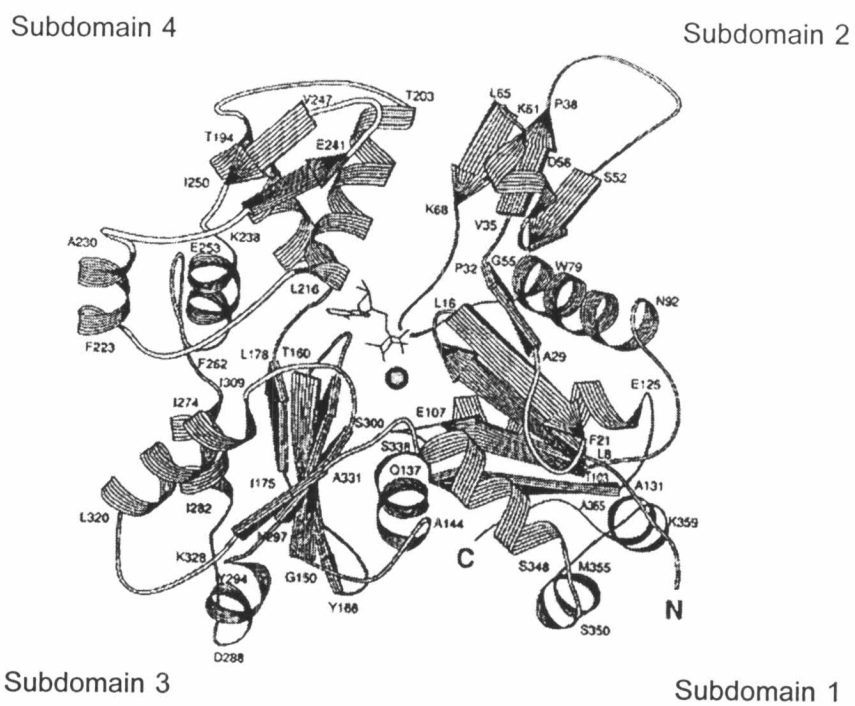

Figure 1 Crystal structure of G-actin. ADP and the metal are located in the cleft between subdomains 1 and 3 (Lorenz et al., 1993).

Monomeric actin (G-actin) readily polymerizes to form filamentous actin under physiological conditions. F-actin is a double helical polymer that has a barbed (+) end and a point (-) end based on the decoration of meromysin to create the arrowhead pattern (Figure 2) (Small et al., 1978; Pollard and Borisy, 2003).

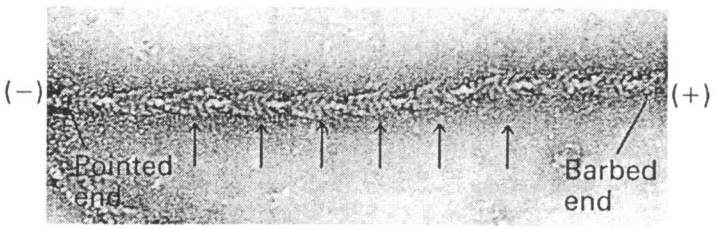

Figure 2 Electron micrograph demonstrates the actin filament decorated with myosin S1 head. The polarity in decoration defines as a pointed (-) end and a barbed (+) end (Lodish et al., 2003).

Actin filaments are dynamic structures; they undergo assembly and disassembly to both ends but the monomers' addition are more rapid at the (+)-end. ATP-actins are further hydrolysed within the filament to form long-lived ADP-actins. At the steady state, ADP-actin monomers are released from (-) end of the filament at the same rate as new ATP-actin monomers are added at the (+) end (Figure 3) (De La Cruz and Pollard, 2001; Pollard and Borisy, 2003).

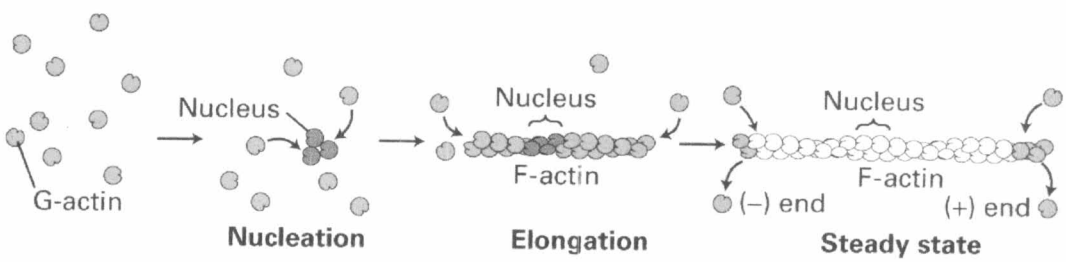

Figure 3 Actin filament elongation (Lodish et al., 2003).

In situ the polymerization-depolymerization of actin is controlled by the actin-binding proteins, which include the monomer sequestering proteins, filament capping proteins, filament severing proteins, and filament cross-link proteins. The monomer sequestering proteins such as thymosin β4 and profillin (Schutt et al., 1993; Sun et al., 1996) act as the G-actin buffering in cytoplasm. Capping proteins that include tropomodulin at the pointed (-) end, CapG, gelsolin, and capping protein at the barbed (+) end bind to filament and block further growth of filament (Barkalow et al., 1996; Cooper and Schafer, 2000; Allen, 2003; Mejillano et al., 2004). The model of actin polymerization that promotes cellular locomotion is shown in Figure 4 (Pollard, 2003).

Moreover, there are some natural toxins that bind to actin (Figure 5). Phalloidin, a bicyclic heptapeptide toxin of the mushroom *Amanita phalloides*, was present in a 2:1 molar excess over actin. Phalloidin binds tightly all along the sides of actin filaments, does not bind to monomeric actin, and stabilizes them against depolymerization (Cooper, 1987; Forscher and Smith, 1988). Cytochalasin D, a fungal alkaloid, binds to (+) ends of actin filaments and prevents elongation (Fox and Phillips, 1981; Cooper, 1987; Forscher and Smith, 1988). Latrunculin A is a toxin from the marine sponge *Latrunculia magnifica* that binds to G-actin monomers and prevents them from polymerizing into filaments (Groweiss et al., 1983; Spector et al., 1983; Coue et al., 1987; Yarmola et al., 2000). Jasplakinolide is a metabolite from the marine sponge *Jaspis johnstoni*. This compound induces actin polymerization by stimulating actin filament nucleation. It stabilizes F-actin and competitively binds to F-actin with phalloidin (Bubb et al., 1994; 2000).

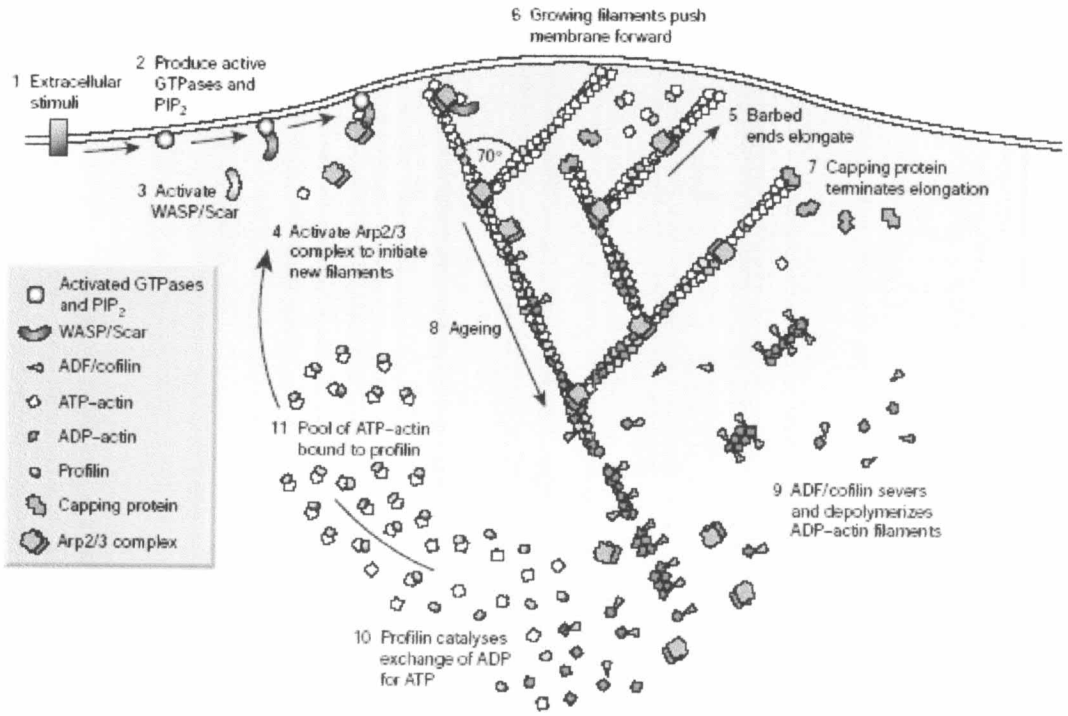

Figure 4 The dendritic-nucleation model for protrusion of lamellipodia.

External cues (1) activate signalling pathways that lead to GTPase (2). These then activate Wiskott-Aldrich syndrome protein (WASP) and related proteins (3), which in turn activate actin-related protein2/3 (Arp2/3) complex. Arp2/3 complex initiates a new filament as a branch on the side of an existing filament (4). Each new filament grows rapidly (5), fed by a high concentration of profiling-bound actin stored in the cytoplasm, and this pushes the plasma membrane forward (6). Capping protein binds to the growing ends, terminating elongation (7). Actin-depolymerizing factor (ADF)/cofilin then severs and depolymerizes the ADP filaments, mainly in the older regions of the filaments (8, 9). Profilin re-enters the cycle at this point, promoting dissociation of ADP and binding of ATP to dissociated subunits (10). ATP-actin binds to profiling, refilling the pool of subunits available for assembly (11) (Pollard, 2003).

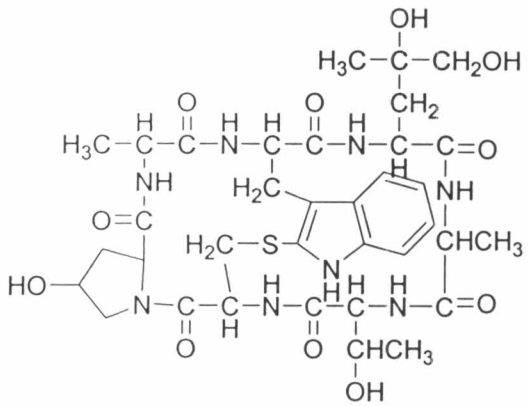

Phalloidin

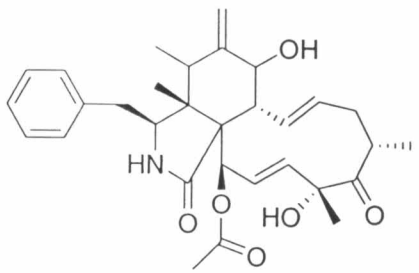

Cytochalacin D

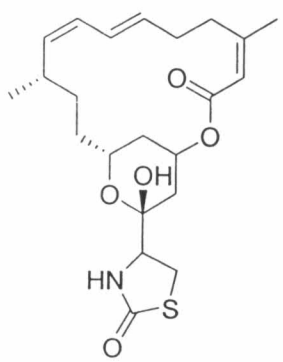

Latrunculin A

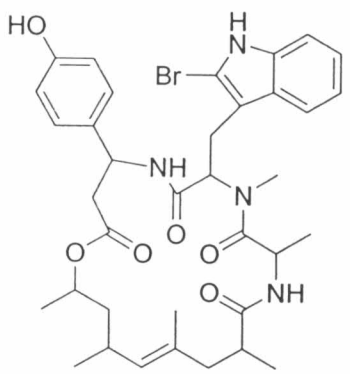

Jasplakinolide

Figure 5 The structures of natural toxins that bind to actin.

5. The structure of kabiramide C-G-actin complex

In 2003, Klenchin et al. presented the X-ray structure of kabiramide C-G-actin complex. This study reveals the absolute configuration of kabiramide C, the binding site of kabiramide C to G-actin, and the proposed mechanism of action of kabiramide C.

The structure of the Ca-ATP form of G-actin in a complex with kabiramide C was determined by molecular replacement to 1.45 Å resolution. The perspective view of the X-ray model for kabiramide C is shown in Figure 6 and the absolute configuration

of kabiramide C was assigned as 3*S*, 5*R*, 7*S*, 8*S*, 9*R*, 22*S*, 23*R*, 24*S*, 26*S*, 27*S*, 31*R*, 32*R*, and 33*R*.

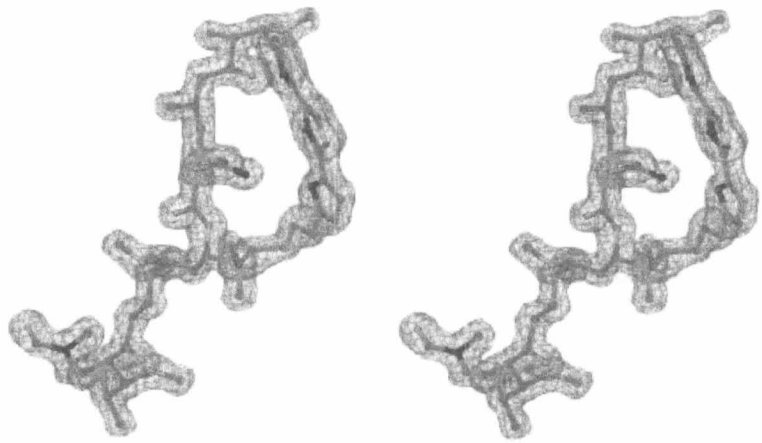

Figure 6 Stereo view of the electron density for kabiramide C (Klenchin et al., 2003).

The structure of kabiramide C-G-actin complex (Figure 7A) reveals that kabiramide C binds in the cleft between actin subdomains 1 and 3. The hydrophobic contacts involving two distinct structural moieties in kabiramide C molecule: (1) the trisoxazole macrolide ring is firmly attached to surface of actin at the interface of subdomains 1 and 3 through a hydrophobic patch formed by Ile341, Ile345, Ser348, and Leu349; and (2) the long aliphatic tail binds deeply within the cleft between subdomains 1 and 3, forming hydrophobic contacts at residues Tyr143, Gly146, Thr148, Gly168, Tyr169, Leu346, Leu349, Phe352, and Met355. The conserved water molecules further stabilize the interaction of the tail with actin by bridging the terminal oxygen of *N*-methyl formamide group and the backbone amide hydrogens of Tyr133, Ile136, and Ala170 (Figure 7B). Moreover, the trisoxazole moiety of the macrolide ring is not planar but bent slightly, as a result of its interaction with actin (Klenchin et al., 2003; Tanaka *et al.*, 2003). The conformational structure of actin in the complex is similar to previous reports (Kabsch et al., 1990; McLaughlin et al., 1993; Schutt et al., 1993; Otterbein et al., 2001; 2002), indicating that kabiramide C does not cause major conformational change in actin.

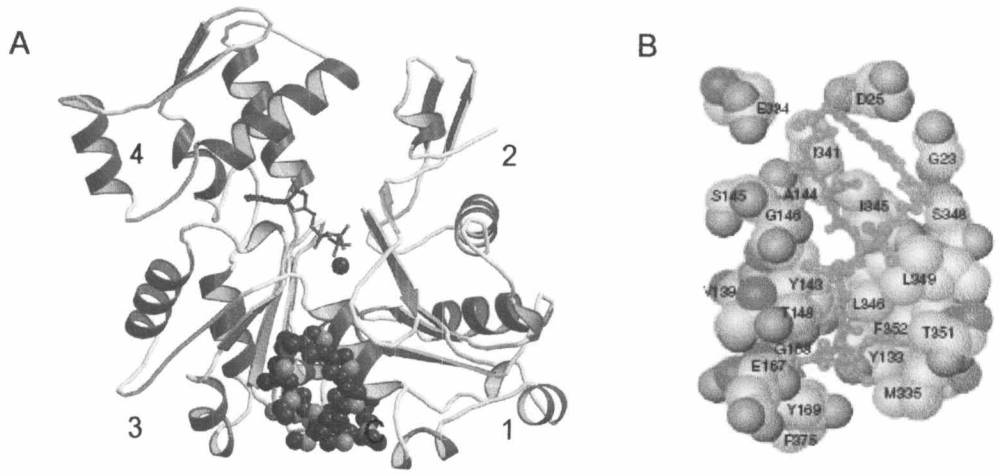

Figure 7 The structure of kabiramide C-G-actin complex. (A) The structure of kabiramide C-G-actin complex, kabiramide C is shown in a space-filling model in red, black, and blue and actin is shown in a ribbon representation. (B) Kabiramide C binding site on actin, kabiramide C is shown in cyan color as ball and stick and labeled amino acid residues contacting kabiramide C are shown in CPK color as space-filling model (Klenchin et al., 2003).

Investigation of the binding site of kabiramide C on G-actin using X-ray crystallography and fluorescence spectroscopy (Klenchin et al., 2003; Tanaka et al., 2003) shows that the binding site of kabiramide C is almost identical to that of gelsolin (actin-binding protein) domain 1 (Figure 8). These studies show that kabiramide C and gelsolin bind to actin using common contact residues on the surface between subdomains 1 and 3 and act as small molecule biomimetic of gelsolin that severing the actin filament and remain tightly bound to barbed (+) end of the filament that cap or block further growth from this end (Janmey et al., 1985).

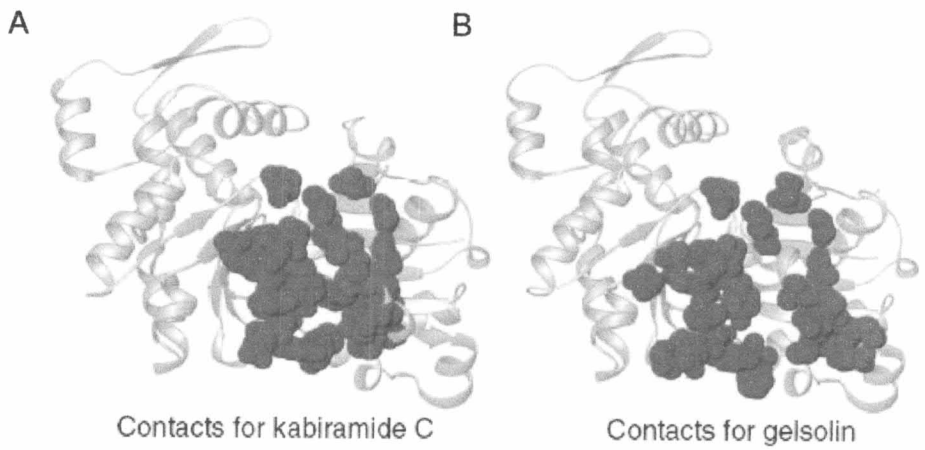

Figure 8 Space-filling representation of the residues on actin that interact with kabiramide C **(A)** and gelsolin domain 1 **(B)** (Klenchin et al., 2003).

The different binding modes of kabiramide C to monomeric actin and actin protomers in a filament are shown in Figure 9. These binding modes of kabiramide C inhibit actin filament dynamics through distinct mechanisms:

(A), Monomer sequestering; kabiramide C sequester actin monomers and raise the critical concentration for actin polymerization.

(B), Barbed (+) end filament capping; the stable kabiramide C-G-actin complex can incorporate onto the (+)-end of an elongating actin filament but kabiramide C in the (+) end bound protomer blocks further addition of actin monomer onto the filament.

(C), Filament severing; kabiramide C binds to actin protomers in the filament and sever the filament at that site.

Analysis of the crystal structure of kabiramide C-G-actin suggests that the substitutions of side groups in the macrolide ring are almost exposed to the solvent and should not affect the interaction with actin. In contrast, elimination of methyl and methoxy groups or introduction of charged or bulky groups on the tail should reduce the strength of interaction.

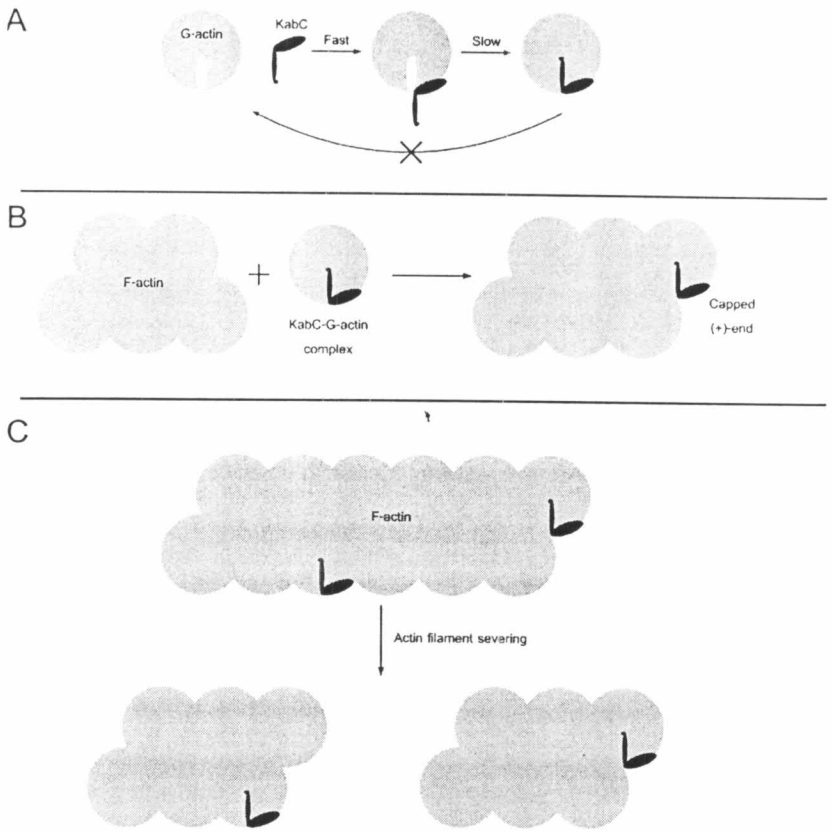

Figure 9 The model of mechanism of action of kabiramide C (KabC).

(A) Sequestering at stoichiometric concentrations of KabC to G-actin. The binding of KabC to G-actin is a two-step reaction with a fast step involving the macrolide ring and a slow step involving the binding of the tail.

(B) (+)-End capping. The strongly bound KabC actin incorporates onto the (+) end of an actin filament but caps further growth.

(C) Filament severing. KabC binds to actin protomers in the filament, where it competes for the site between subdomains 1 and 3 with the axial actin protomer. Once the drug is fully bound, it severs the filament and caps the new (+)-end. (Image based on an original Figure from Klenchin et al., 2003).